

Novel Designed CSRRs and Its Application in Tunable Tri-Band Bandpass Filter Based on Fractal Geometry

He-Xiu XU, Guang-Ming WANG, Jian-Gang LIANG

Missile Institute of Air Force Engineering University, Sanyuan 713800, China

hxxu2008@yahoo.cn, Wgming01@sina.com, cat-liang1975@163.com

Abstract. *In this paper, we propose and research a novel miniaturized composite right/left handed transmission line (CRLH TL) cell based on revised complementary split ring resonators (CSRRs) for the first time. Novel CRLH TL cell is demonstrated with lower transmission and reflection zeros from electrical and electromagnetic (EM) simulation results. Negative refractive index of CRLH effect is successfully demonstrated by the revised NRW retrieval method. Then based on this, a tri-band bandpass filter (BPF) is synthesized and fabricated by using the proposed CRLH TL cell (providing the primary GSM band) and Koch fractal-shaped microstrip line (ML) (generating the upper GPS and ISM bands). Our recent work has also found that open-circuit stub embedded in Koch-shaped ML can be optimized to adjust the ratio of the upper two bands, thus afford us additional flexibility in BPF design. Consistent result obtained from simulation and measurement is presented which have verified the design concept.*

Keywords

Miniaturization, bandpass filter (BPF), composite right/left handed transmission line (CRLH TL), complementary split ring resonators (CSRRs), tri-band, fractals.

1. Introduction

Wireless multi-standard communication has generated much of interest in recent years. Various wireless standards including mobile communication band (GSM) (800/900 MHz), global position system band (GPS) (1570 MHz), and Industrial, Scientific and Medical (ISM) (2.4/5.2 GHz) band have emerged in the communication industry. In order to fulfill the increasing requests and demands in this field, a mass of previous works and research are implemented in the design of multiband especially for tri-band devices or systems, e.g., tri-band transceiver reported in [1], tri-band antenna [2], [3], and finally but not the last, tri-band bandpass filters (BPFs) [4-6] for commercial practical application.

Above-mentioned tri-band BPFs exhibit many advantages such as compact in size [4], sharp rejection skirts [5], [6], however, the virulent drawback, e.g., large insertion loss [5], [6] deserves further improvement. Fractal theory

has been widely utilized in the design of microwave components based on its space-filling and self-similarity nature, which makes the compact, multiband [7], or improved pass-band performance [8] design possible. In view of it, a novel tri-band BPF constructed by Koch-shaped microstrip line (ML) (providing the upper two bands) and CRLH TL cell (providing the primary band) is proposed. The paper is well organized as follows. In section 2, we present a novel CSRRs and its corresponding equivalent circuit model first. Then the miniaturization principle is disclosed during the lumped parameters extraction process. Finally the refractive index behavior of the proposed structure is emphasized by performing a constitutive parameters extraction based on the revised NRW retrieval method, which constitutes an essential contribution of this paper. Section 3 provides the application of the CSRRs in BPF based on the Koch-shaped ML as well as simulated and measured results. Finally, the main conclusion is highlighted in section 4.

2. Novel CSRRs and Analysis

2.1 Proposed Structure, Equivalent Circuit Model and Miniaturization Principle

Novel designed complementary split ring resonators (N-CSRRs) outlined in Fig. 1(a) with the inner and outer ring connected configuration, initially adopted in split ring resonators (SRRs) design to realize negative permeability [9], is firstly employed in the design of miniaturized CRLH TL cell to fulfill negative permittivity. Conventional CSRRs (see Fig. 1(b)) is putted forward in terms of comparison. Equivalent T-circuit model depicted in Fig. 1(c) for conventional CSRRs is also appropriate for N-CSRRs. In this model, whereas L_s models the line inductance, C_g represents gap capacitance, C is composed of the line capacitance and the coupling capacitance between the conductor line and the N-CSRRs, parallel resonant tank L_p and C_p is employed to model the complex effect of N-CSRRs. Additional ML_p is associated to compensate the parasitical effectiveness of right handed (RH) ML extended to termination port.

Concentrate on the innovative configuration of SRRs, the capacitance C_p are four times of conventional SRRs [9]. However, considering the Babinet principle, it can be easily

achieved that the inductance L_p of the N-CSRRs should be four times of conventional one. This can be successfully interpreted as: L_p for N-CSRRs case equal to two identical inductances in series while in parallel for common CSRRs case by contrast. According to classical circuit theory, the transmission zero and resonance frequency of CSRRs (approximately equals to in-band reflection zero) read as

$$\begin{aligned} f_T &= 1/2\pi\sqrt{L_p(C+C_p)} \\ f_r &= 1/2\pi\sqrt{L_p C_p} \end{aligned} \quad (1)$$

Thus the transmission and reflection zeros of N-CSRRs can be theoretically predicted as half of conventional one.

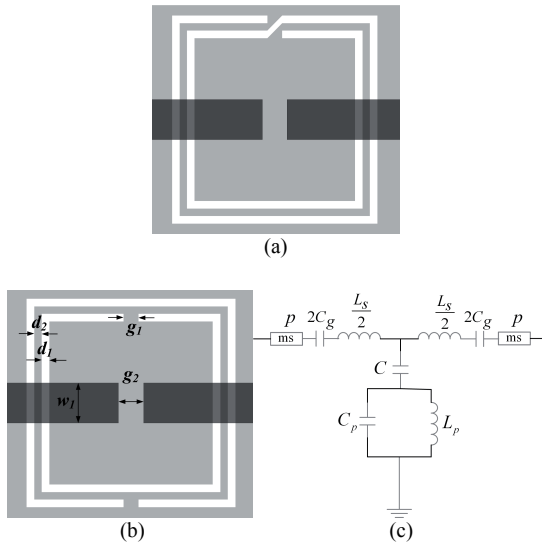


Fig. 1. CRLH TL cells constructed by CSRRs (denoted in white) etching in the ground plane (denoted in light grey) and capacitive gap embedded in the conductor strip line (denoted in dark grey): (a) proposed N-CSRRs; (b) conventional one; (c) lumped elements equivalent T-circuit model of correlative CRLH TL cells, where $d_1 = 0.3$ mm, $d_2 = 0.3$ mm, $g_1 = 0.6$ mm, $g_2 = 1$ mm, $w_1 = 1.6$ mm.

The substrate with dielectric constant (ϵ_r) of 2.65 and thickness (h) of 0.8 mm is used for all designs in this paper. To validate the effectiveness of the proposed equivalent T-circuit model as well as rationality and exactness of analysis discussed above, electromagnetic (EM) simulation through *Ansoft Designer* has been implemented. We also perform a lumped parameters extraction for electrical simulation through *Ansoft Serenade*. In this process, equivalent T-circuit model is applied in *Serenade* to determine the lumped parameters by matching the S parameters of the circuit model to the EM simulated ones. Extracted lumped parameters for both CSRRs-based CRLH TL cells are analyzed and compared in Tab. 1. By consulting the values of lumped elements, we can evidently draw the conclusion that L_p of N-CSRRs is approximately four times of conventional CSRRs while almost without any variation of values of other lumped elements.

Fig. 2 plots the comparison of S-parameters of these CRLH TL cells between EM simulation and electrical simulation. Good agreement can be observed in the whole

frequency range which has confirmed the rationality of the proposed circuit model. It also can be acquired from Fig. 2 that transmission and reflection zeros (0.43 and 1.2 GHz) of N-CSRRs-based cell are nearly half of conventional ones (0.86 and 2.36 GHz) and simultaneously with almost identical RH band (centered at 6.1 GHz) for both cases. Hence revised CSRRs structure affects left handed (LH) band in the mechanism of changing the value of L_p while without any influence to RH band. Furthermore, N-CSRRs-based CRLH TL cell with electrical dimension only $0.048\lambda_g$ is mostly preferred for miniaturization application, where λ_g is the wavelength of center frequency in LH band.

CRLH TL type	L_s (nH)	C_g (pF)	C (pF)	L_p (nH)	C_p (pF)	P (mm)
N-CSRRs	6.8	0.105	8.04	20.2	0.425	2.63
CSRRs	7.4	0.1	8.57	5.2	0.45	3

Tab. 1. Extracted lumped parameters for both CSRRs-based CRLH TL cell.

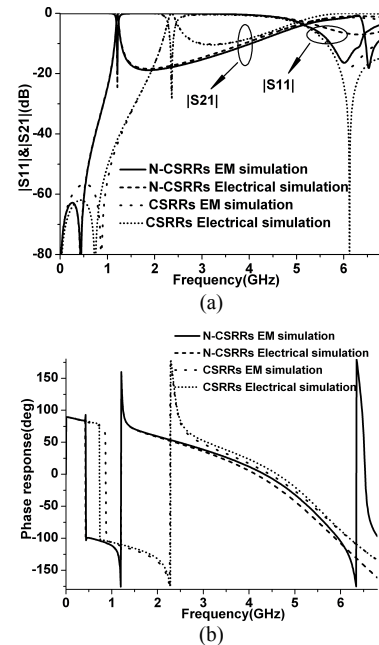


Fig. 2. S-parameters of the CSRRs-based CRLH TL cells described in Fig. 1: (a) return and insertion loss $|S_{11}|$ & $|S_{21}|$; (b) phase response.

2.2 Effective Constitutive Parameters Extraction

In order to prove that the N-CSRRs-based cell is still a resonate-type CRLH TL, a improved retrieval method using S-parameters based on Nicolson–Ross–Weir (NRW) approach [10], [11] is applied during the effective constitutive parameters extraction process, in which we adopt a mathematical method used by X.-D Chen et al [12] to choose the correct branch of the real part of the refractive index for robustness. Fig. 3 provides results of the effective permeability μ_{eff} and permittivity ϵ_{eff} . It can be observed that both permeability and permittivity exhibit simultaneously negative real parts around the resonance frequency 1.2 GHz,

thus a LH band exists in the vicinity of 1.2 GHz (see Fig. 2). Otherwise there is a stopband provided any single negative real part of permeability and permittivity, e.g., from 1.35 to 5.2 GHz, the real part of ϵ_{eff} is obtained as positive values while μ_{eff} negative ones. By contrast, with the frequency range of above 5.2 GHz, we emphasize that both real part of ϵ_{eff} , μ_{eff} have positive values, consequently a RH band is obtained.

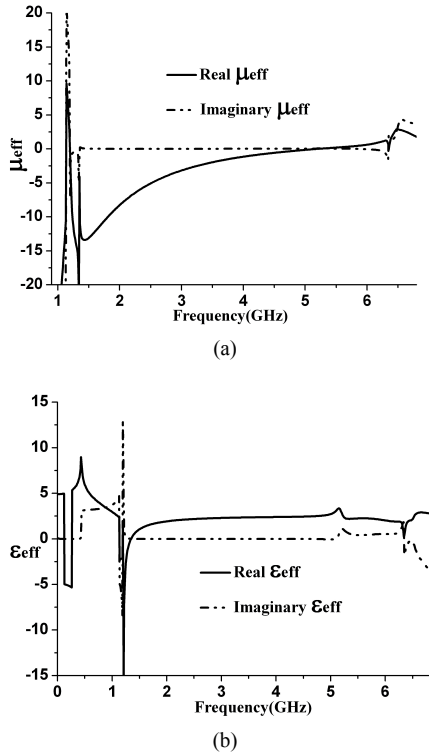


Fig. 3. Constitutive effective parameters of the proposed structure (a) permeability μ_{eff} , (b) permittivity ϵ_{eff} .

From the computed refractive index n and propagation constant β plotted in Fig. 4, we should highlight that both real part of n and β obtained as negative values within approximately the identical frequency range. The refractive

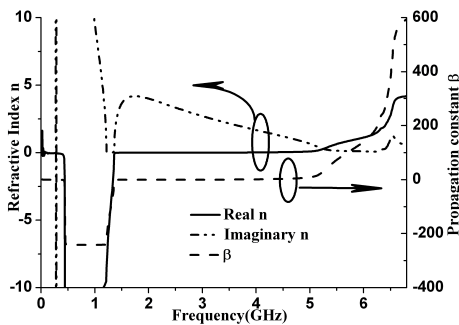


Fig. 4. Refractive index n and propagation constant β . Note that the frequency band of negative real parts of n and β agree well with each other.

indexed band (ranged from 0.4 to 1.37 GHz) is achieved even wider when relative to the EM-simulated 3-dB pass-band (ranged from 1.19 to 1.3 GHz), which seemingly makes us believe that both results are in conflict with the each other. But in practice, a careful look-in in the imagi-

nary part of n , one can easily find that these values are much larger than zero and shifting sharply from 0.4 to 1.19 GHz, which indicates an inhibition of signal propagation to some degree. Moreover, negative propagation constant of β have confirmed the backward wave transmission. Successful retrieval results demonstrate not only the effectiveness and robustness of the extraction method but also the CRLH effect of the proposed CSRRs.

3. Tri-Band BPF Application and Illustrative Results

In this section, we consist on constructing two N-CSRRs-based CRLH TL cells discussed above in the Koch-shaped ML to synthesize a tri-band filter (with topology outlined in Fig. 5). Koch-shaped ML determined by the iteration factor ($IF = 1/3$) and iteration order ($IO = 2$) is considered for providing the two upper bands due to the self-similarity of fractal nature. Open-circuit stub embedded in the interspace of ML is from the point of adjusting the location of the upper two bands. Our experimental works have found that the open-circuit stub employed in the BPF design can affect the ratio of upper two bands, thus afford us additional flexibility in BPF design. Two CRLH TL cells utilized in this work are aimed to generate the primary first band (GSM band) and improve out-of-band suppression and selectivity to some degree. What's more, stepped-impedance configuration for CTLH TL cell is taken into account bandwidth enhancement and miniaturization. As the low-impedance section (broader width) of ML above CSRRs induces a larger coupling capacitance C , which further reduces the transmission zero according to (1). Detailed physical parameters are optimized and given in Fig. 5. For verification of the simulation results, the designed BPF is fabricated and measured. Fig. 6 plots the fabricated prototype of the designed tri-band BPF. Novel designed BPF is compact in size whose effective occupied area is $54 \times 27.6 \text{ mm}^2$.

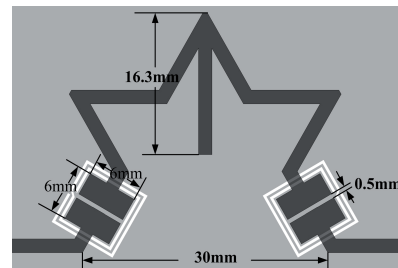


Fig. 5. Topology of the proposed tri-band BPF.

Fig. 7 exhibits the simulated (characterized by *Ansoft Designer*) and measured (characterized by *Anritsu ME7808A* vector network analyzer) frequency response of the proposed tri-band BPF. Good agreement can be observed in the whole frequency region of interest. The measured -10dB return loss frequency ranged for the three passbands centered at f_1 , f_2 , and f_3 are found to be 890–1100 MHz (12.5%), 1500–1570 MHz (4.5%), and 2360–2450 MHz (3.7%) respectively. Minimum insertion

loss measured for these three passbands in the same sequence are 0.21, 0.45, and 0.6 dB accordingly which are very comparable with regard to the already covered tri-band BPFs whose largest minimum insertion loss is 1.8 dB in [5] and 3 dB in [6].

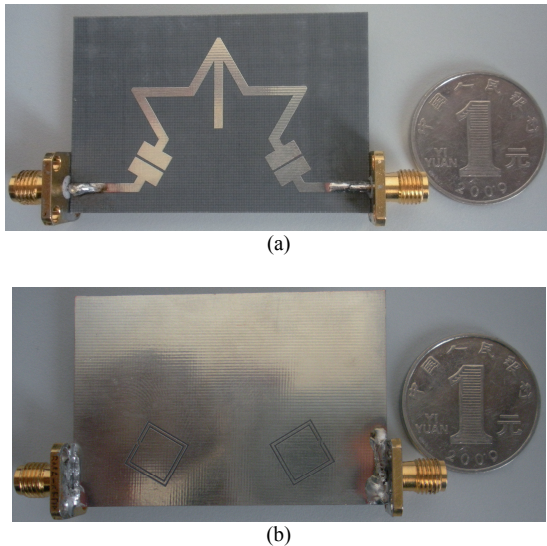


Fig. 6. Fabricated prototype of the designed tri-band BPF: (a) top view; (b) bottom view.

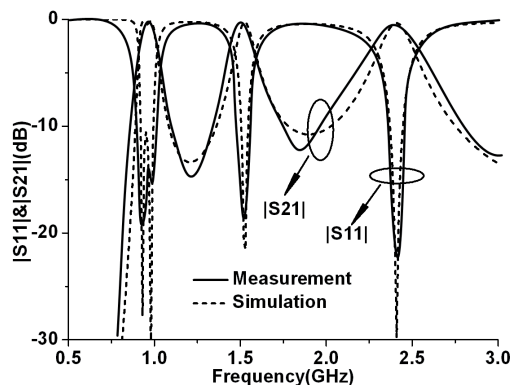


Fig. 7. Frequency response of the designed tri-band BPF.

The primary first band is found mainly depending on the physical parameters of the CSRRs, which provide us clear guidelines to locate it. As to upper two bands, although there is no clear formula derived for design, we have found the generation mechanism of two bands, i.e., the second band mainly depends on the dimension of fractal-shaped ML provided that the IF and IO maintain constant, by contrast, the third band depends on not only the dimension of fractal-shaped ML but also the length and width of the open-circuit stub. Thus for convenience, we can design the third band just by tuning the physical parameters of the stub when the lower two bands have been determined. Derivation of exact design formula or relationship between entitle physical parameters with the three bands are very tedious or even impossible due to the complex interrelation of them. So the roughly obtained design guidelines are very essential in the exactly locating the three bands.

4. Conclusions

A new tri-band BPF using novel miniaturized CSRRs and fractal-shaped ML have been proposed to provide three commercially practical passbands covered 900 MHz, 1570 MHz, and 2400 MHz. The transmission and reflection zeros of CRLH TL based on N-CSRRs are found to be half of conventional one. Therefore it is very suitable for electrically small devices design. The proposed structure with negative refractive index and propagation constant is validated to be a CRLH TL metamaterial. Advantages of the BPF may be summarized in several aspects: compact in size, low return and insertion loss in passbands, innovative and simple in design and convenient in tuning upper bands through stub. Disadvantages of it mainly exist in relatively narrow bandwidth of upper two bands which should be pursued in future work.

Acknowledgements

This work is supported by the National Natural Science Foundation of China under Grant Nos. 60971118. The authors would like to thank the China North Electronic Engineering Research Institute for the fabrication. Special thanks should be also delivered to the anonymous reviewers for constructive comments.

References

- [1] LIN, Y.-S., LIU, C.-C., LI, K.-M., CHEN, C.-H. Design of an LTCC tri-band transceiver module for GPRS mobile applications. *IEEE Trans. Microw. Theory Tech.*, Dec. 2004, vol. 52, no. 12, p. 2718–2724.
- [2] AZARO, R., ZENI, E., ROCCA, P. et al. Synthesis of a Galileo and Wi-Max three-band fractal-eroded patch antenna. *IEEE Antennas Wireless Propag. Lett.*, 2007, vol. 6, p. 510-514.
- [3] SOON YOUNG EOM, SEONG HO SON, YOUNG BAE JUNG, et al. Design and test of a mobile antenna system with tri-band operation for broadband satellite communications and DBS reception. *IEEE Trans. Antennas Propag.*, Nov. 2007, vol. 55, no. 11, p. 3123-3133.
- [4] CHING-HER LEE, CHUNG-I. G. HSU, HE-KAI JHUANG Design of a new tri-band microstrip BPF using combined quarter-wavelength SIRs. *IEEE Microw. Wireless Compon. Lett.*, Nov. 2006, vol. 16, no. 11, p. 594-596.
- [5] CHUNG-I G. HSU, CHING-HER LEE, YI-HUAN HSIEH Tri-band bandpass filter with sharp passband skirts designed using tri-section SIRs. *IEEE Microw. Wireless Compon. Lett.*, Jan. 2008, vol. 18, no. 1, p. 19-21.
- [6] BO-JIUN CHEN, TZE-MIN SHEN, RUEY-BEEI WU Design of tri-band filters with improved band allocation. *IEEE Trans. Microw. Theory Tech.*, July 2009, vol. 57, no.7, p. 1790-1797.
- [7] KRZYSZTOFIK, W. J. Modified Sierpinski fractal monopole for ISM-bands handset applications. *IEEE Trans. Antennas Propag.*, Mar 2009, vol. 57, no. 3, p. 606-615.
- [8] XU, H. X., WANG, G. M., ZHANG, C. X. Fractal-shaped UWB bandpass filter based on composite right/left handed transmission line. *Electron. Lett.*, 2010, vol. 46, no. 4, p. 285-286.

- [9] WU MING-FENG, MENG FAN-YI, KANG JIA-HUI, et al. Novel miniaturized planar left-handed metamaterial transmission line verified by the backward wave property. *Acta Physica Sinica*, 2008, vol. 57, no. 2, p. 822-826.
- [10] NICOLSON, A. M., ROSS, G. F. Measurement of intrinsic properties of materials by time-domain techniques. *IEEE Trans. Instrum. Meas.*, Nov. 1970, vol. IM-19, no. 4, p. 377-382.
- [11] WEIR, W. B. Automatic measurement of complex dielectric constant and permeability at microwave frequencies. *Proc. IEEE*, Jan. 1974, vol. 62, no.1, p. 33-36.
- [12] XUDONG CHEN, GRZEGORCZYK, T. M., BAE-IAN WU, PACHECO, J. JR., JIN AU KONG Robust method to retrieve the constitutive effective parameters of metamaterials. *Phys. Rev. E*, 2004, vol. 70, 016608.

About Authors ...

He-Xiu XU was born in the Jiangxi province of China. He received his BS degree in communication engineering from the Missile Institute of Air Force Engineering University, Xi'an, China, in 2008 where he is now pursuing his PhD degree. His research interests include metamaterials and

fractals as well as their applications to microwave components and antennas.

Guang-Ming WANG was born in the Shannxi province of China. He received his BS and MS degrees from the Missile Institute of Air Force Engineering University, Xi'an, China, in 1982 and 1990, respectively, and his PhD degree from the Electronic Science and Technology University, Chengdu, China, in 1994. He joined the Air Force Engineering University as an associate professor and was promoted to a full professor in 2000, and is now the head of the Microwave Laboratory center of it. His current interest includes passive and active microwave circuits, antenna and propagation, and also the new structures including EBG, PBG, metamaterials and fractals, etc.

Jian-Gang LIANG was born in the Anhui province of China. He received his BS, MS and PhD degree in the major of electromagnetic field & microwave technology from the Missile Institute of Air Force Engineering University, Xi'an, China, in 1997, 2000 and 2004 respectively. He is now the youngest head of the Microwave Theory and Application Laboratory. His research interests include microwave passive and active circuits and antennas.